The study of warm dense matter: both a servant to and a beneficiary of high aspect laser drilling.

Andrew Forsman and Paul Parks

General Atomics, San Diego, USA

GENERAL ATOMICS

Organization of Presentation

- **The presence of warm dense matter in laser materials processing.**
  - Frequently present
- **Putting warm dense matter to work in laser materials processing.**
  - A role of warm dense matter in the drilling of high aspect ratio holes.
- **A proposed ion beam experiment in structured materials produced by laser micromachining.**
  - The production and probing of "quasistatic" expanded states of matter.
- **Conclusions**

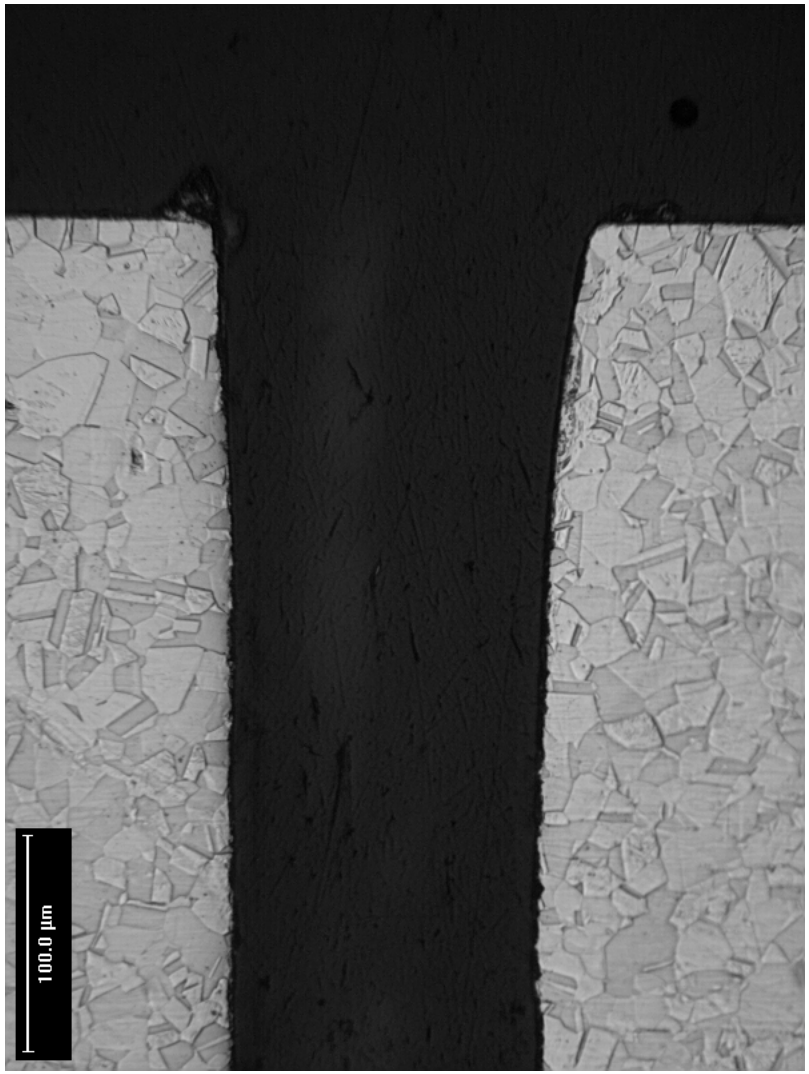

The advent of industrialized short pulsed (fs to ns) lasers brings WMD to the shop floor.

- **Hydrocode provides insight.**
- **Extreme (for LMP) conditions of temperature and pressure.**
  - **T=300,000 K at pulse peak.**
  - **P=60,000 Atmospheres (seen by VISAR)**
- **Units:**
  - Position in m
  - Temperature in eV (1eV=11,000 K)
  - Pressure in kBar (1kBar=1,000 atmospheres)
  - Density in kg/m^3
  - Laser Energy Deposition in 10^{16} W/m^3
    - Shows the expected self-modulation due to interference between the incident and reflected waves.

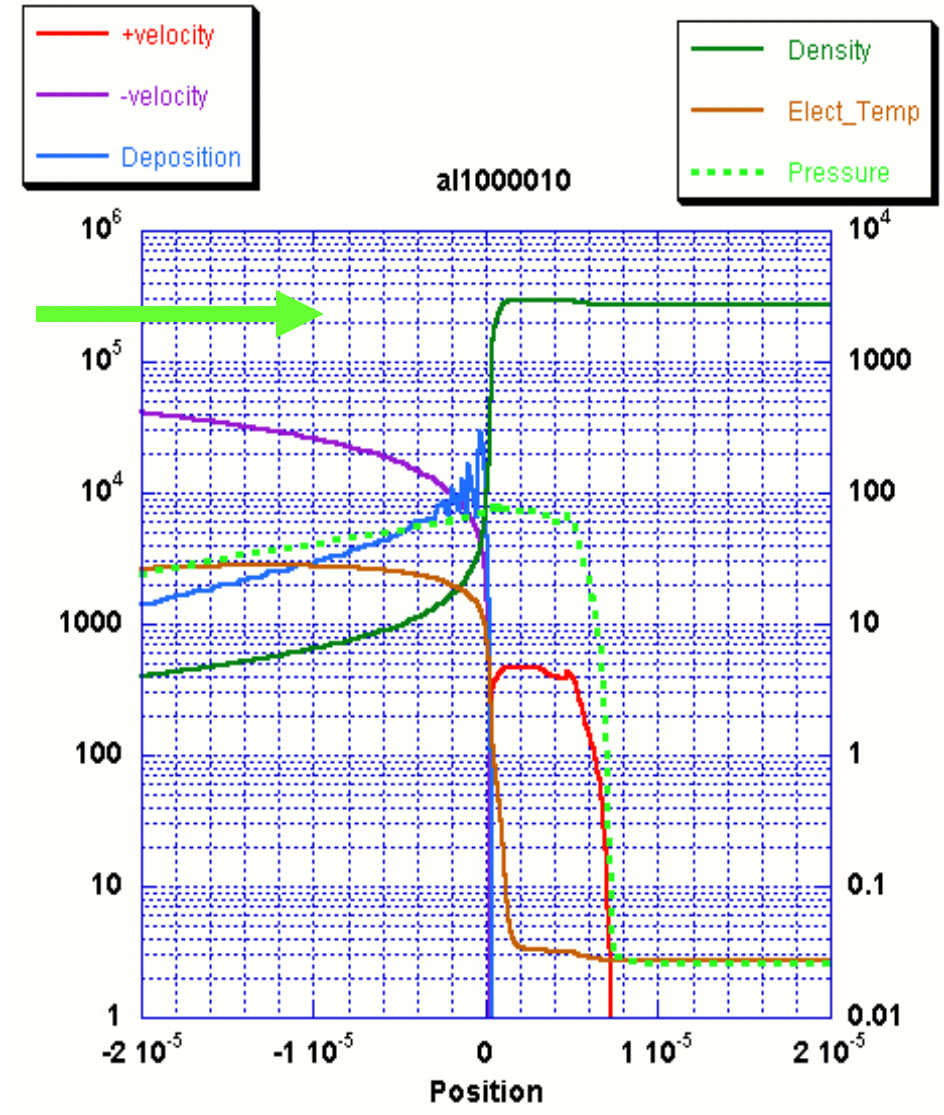

Laser-matter interaction hydrocode simulations reveal the extent of WDM in laser materials processing

- **Finite-element fluid model calculates the evolution of each individual element.**
- **Each individual element represents a layer of target material.**
- **We can track the change of velocity, density, temperature, etc.**

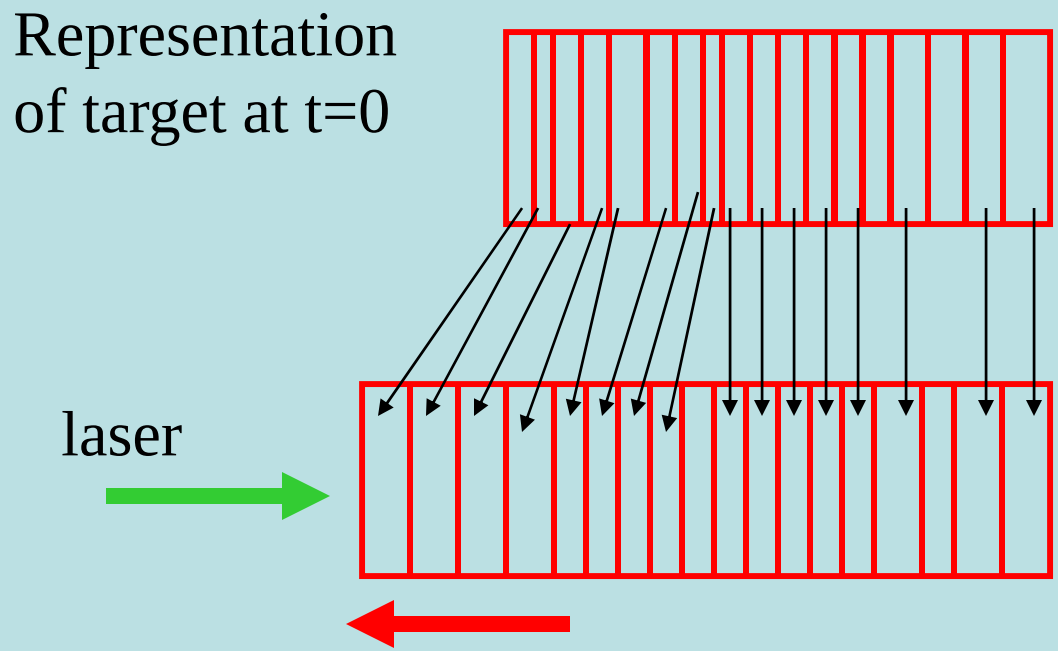

Representation of target once heated by laser (front cells expand and move outward).

Laser machining does not stop with the laser pulse: WDM can be ejected and lingers after the laser pulse.

- **Laser materials processing abhors ablation products.**
  - Ablated material has to go somewhere.

- **Following series show ρ, T for various pulse widths from 1 ps to 100 ns.**
  - 10 ns to 100 ns: boiling material off
  - 1 ns to 10 ns: plasma then denser, cooler phase.
  - 1 ps to 30 ps: plasma then by material ejection due to post-compression target relaxation.

- **Fresh WDM can be ejected long after the laser pulse**
  - LMP does not stop with the laser pulse…

Evolution of target for various depths from surface for a 10 ns FWHM pulse at ~200 J/cm^2 : lots of plasma and some dense, warm matter

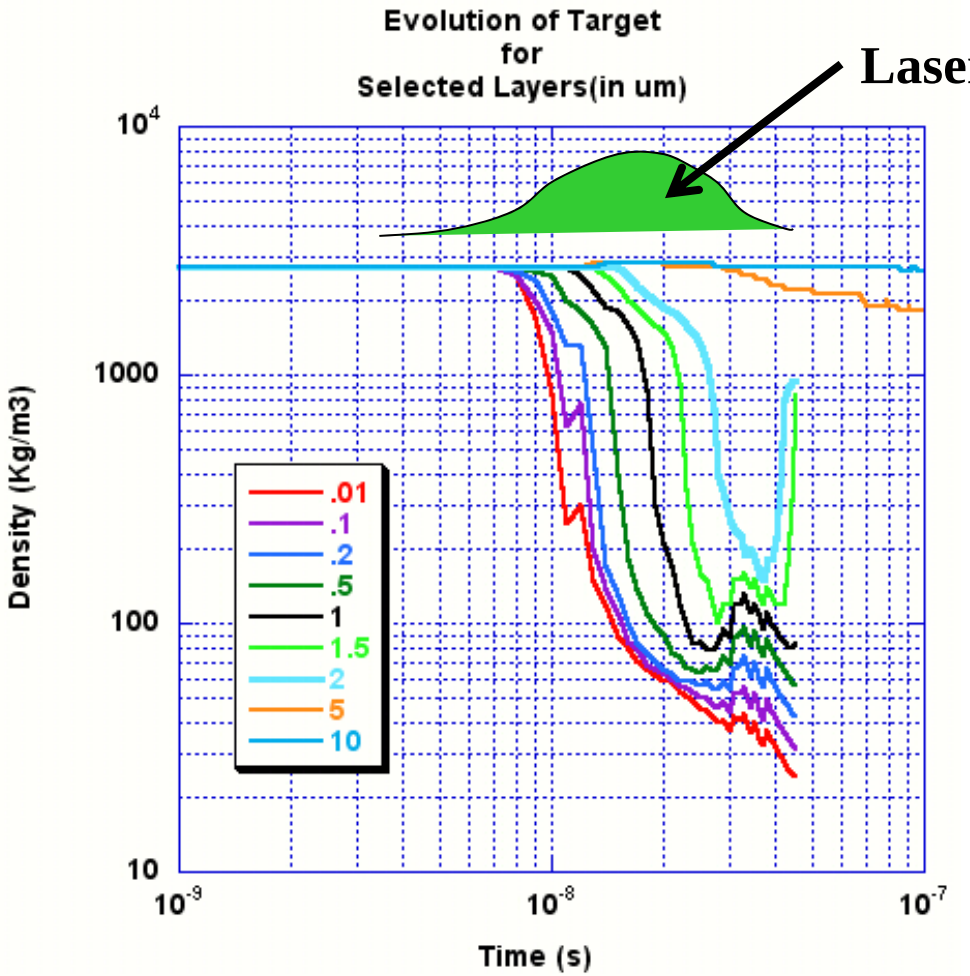

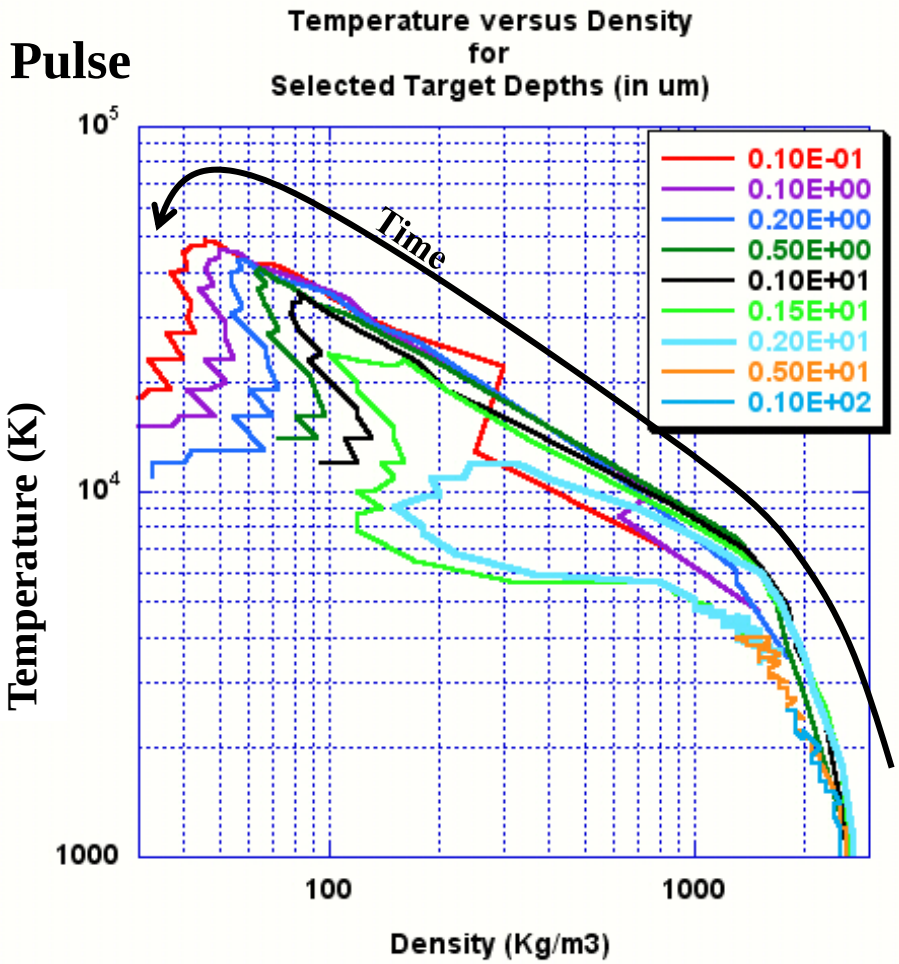

$$\left(2\times10^{10}\,W/cm^2\right)$$

Same energy, 10X shorter (1 ns FWHM) pulse: less plasma, more WDM. More significant WDM "hanging around" target, emerging after pulse

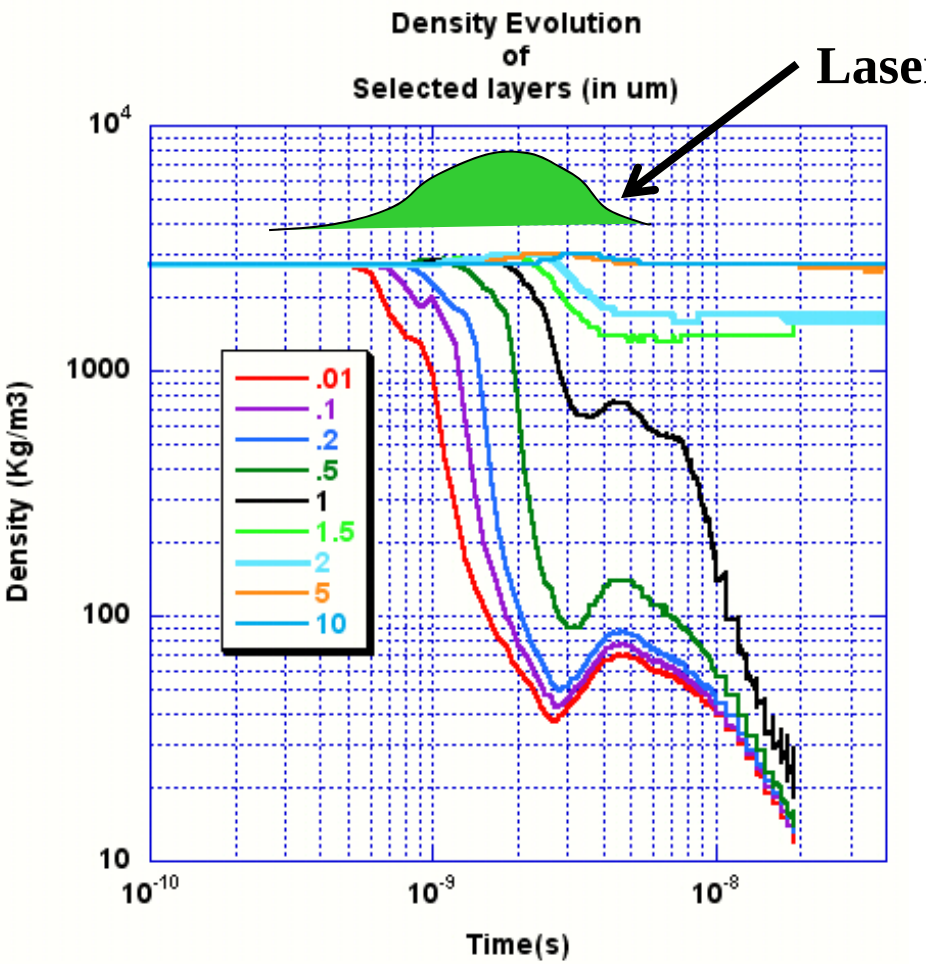

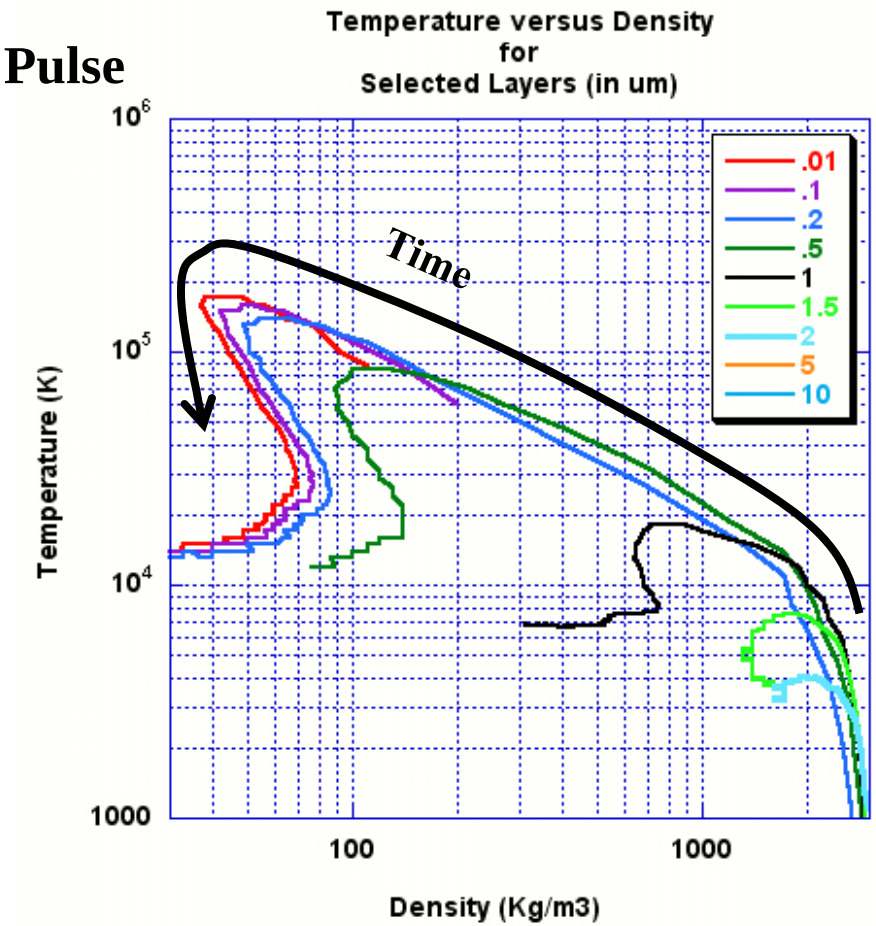

$$\left(2\times10^{11}\,W/cm^{2}\right)$$

And 10X shorter to 100 ps FWHM but same energy: still plasma coupling , now emergence of prominent WDM from post-compression release

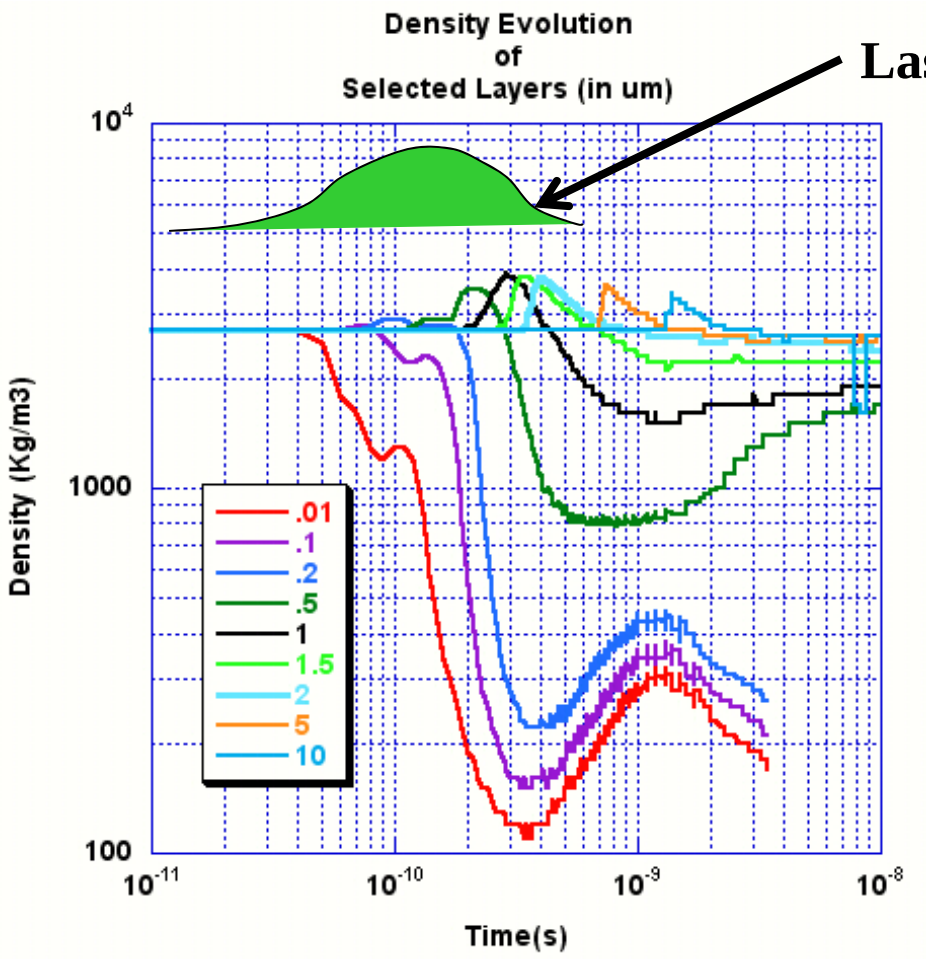

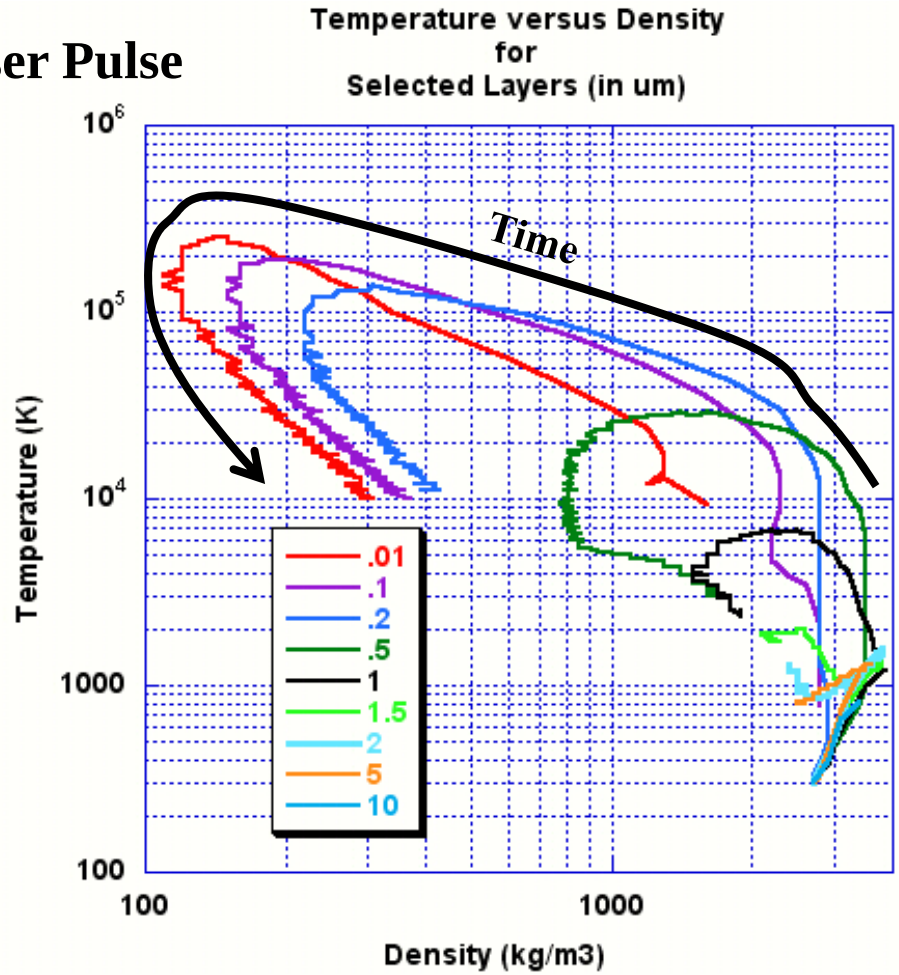

10X shorter again to 10 ps FWHM, at same energy: less plasma but lots of WDM emerging after pulse

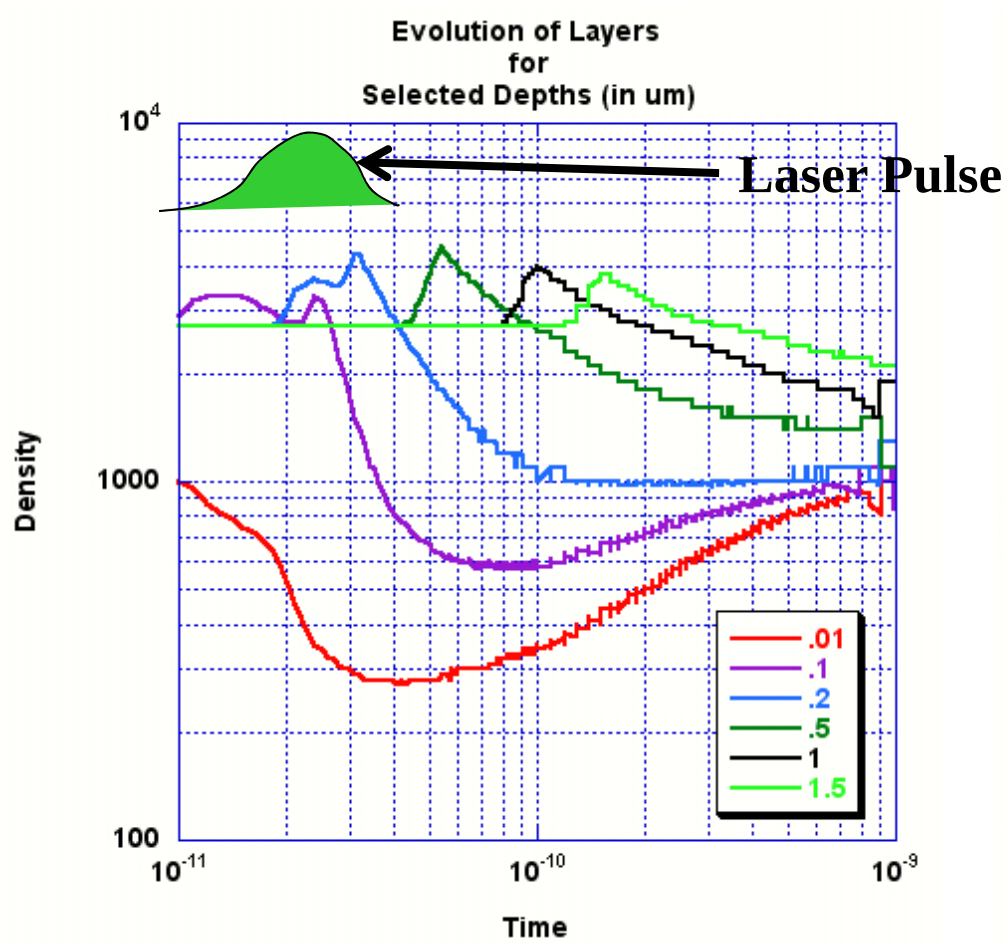

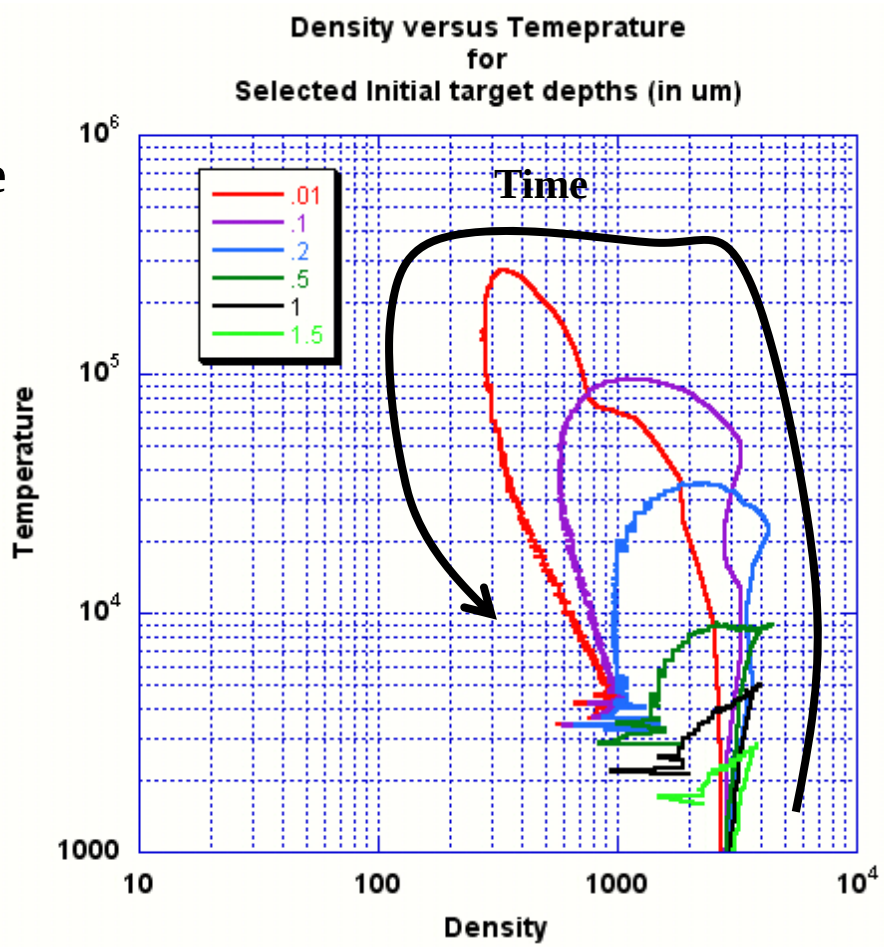

$$\left(5\times10^{12}\,W/cm^2\right)$$

Again 10X shorter to 1 ps FWHM, at same energy:

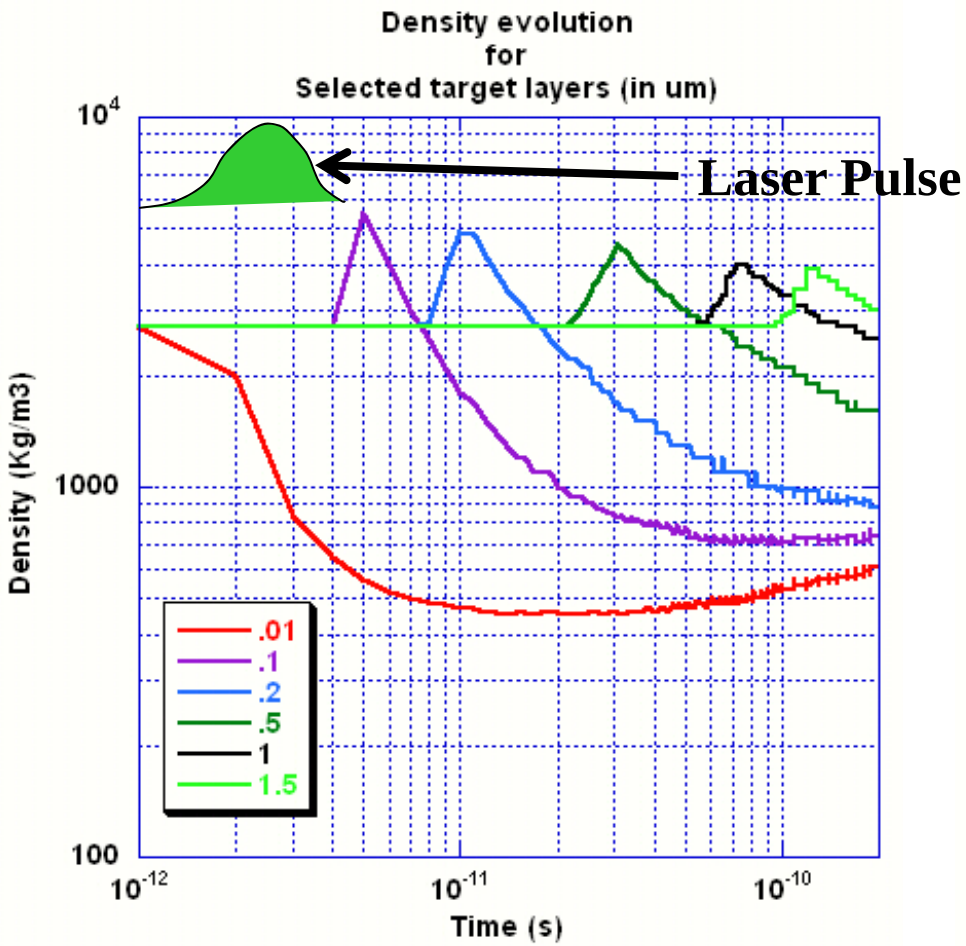

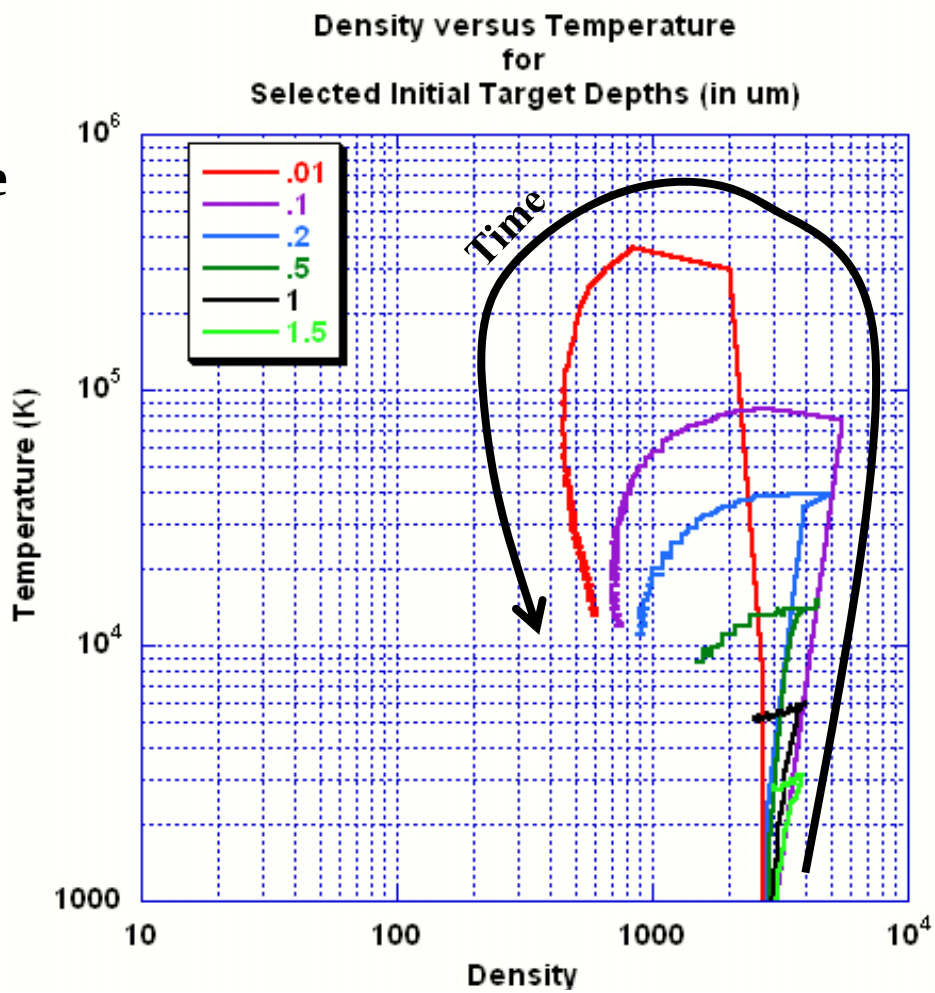

The presence of this hot matter generally has negative implications for hole drilling (for example).

- **Plasma related:**
  - Radial hole expansion by hot plasma
  - Friction encountered by plasma exiting hole
  - Plasma thermal deposition in bore walls
- **Optical phenomena:**
  - Waveguiding
  - Propagation losses
- **Redeposition:**
  - From plasma
  - From liquid and vapor

We only begin to grasp some of these processes.

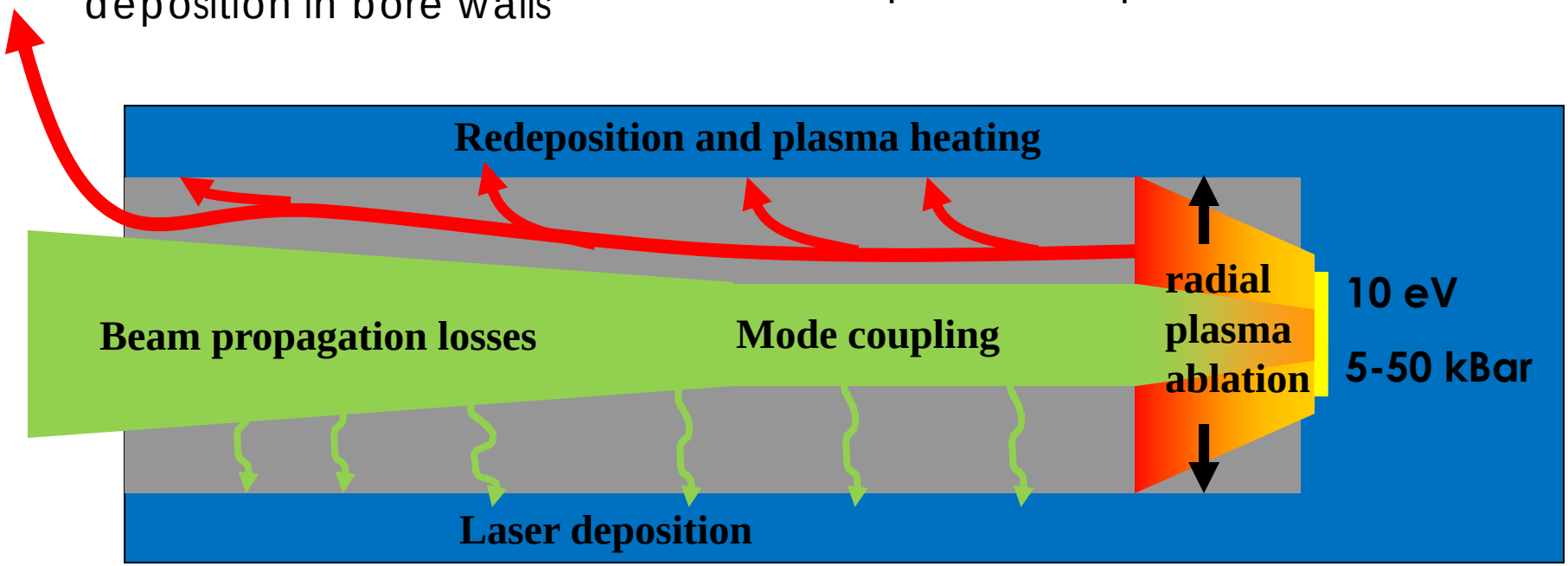

In high aspect ratio laser drilling the plasmas and other ejecta matter.

- **In a small and confined hole, more highly energetic plasmas can enlarge the hole.**
- **Redeposition can block the hole.**
- **Short pulse lasers are not a panacea.**
  - Equivalent energies produce very high energy density.
  - Coupling to higher densities and changing reflectivity

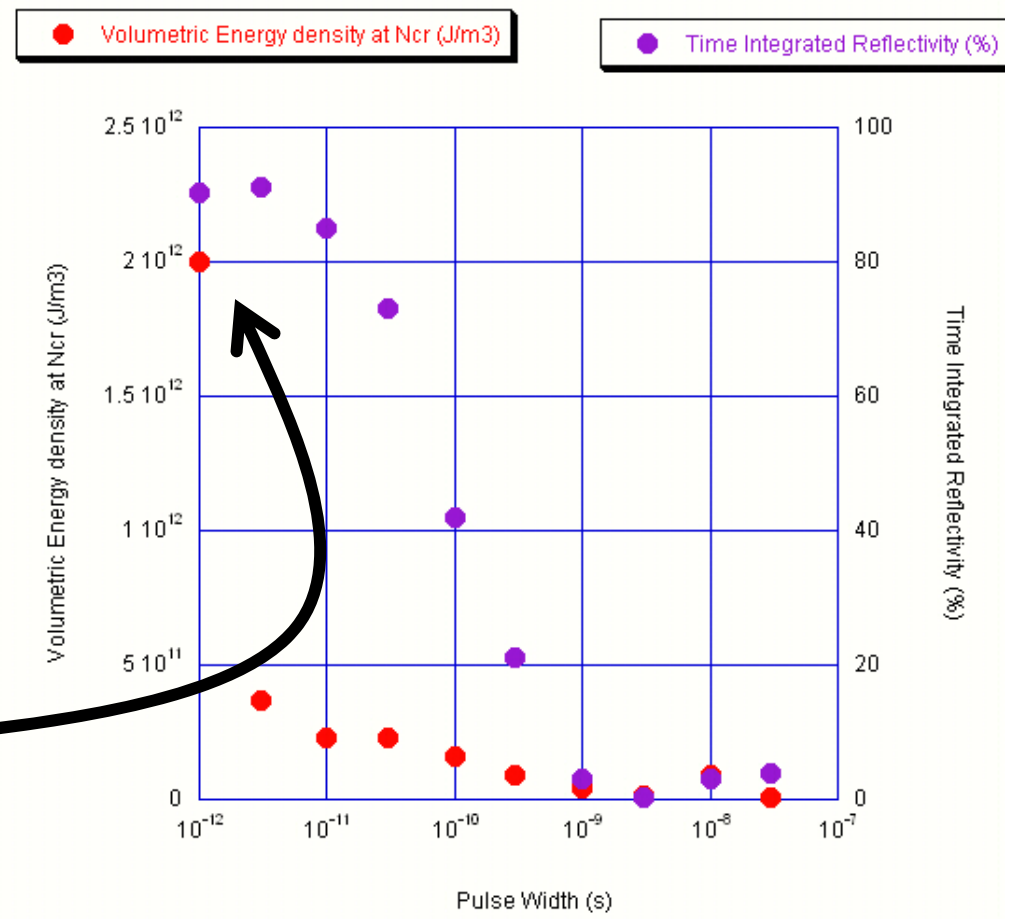

Increasing energy density increases size beyond what can be accounted for optically (nanosecond example)

- **Tests in 150 um thick Al foil reveal that the hole size depends on the laser intensity.**
  - Drilling time is constant at 2000 double pulse laser shots.
  - Focal spot diameter <6um
  - Low taper in holes.
  - *Ablation plasma causes radial ablation*

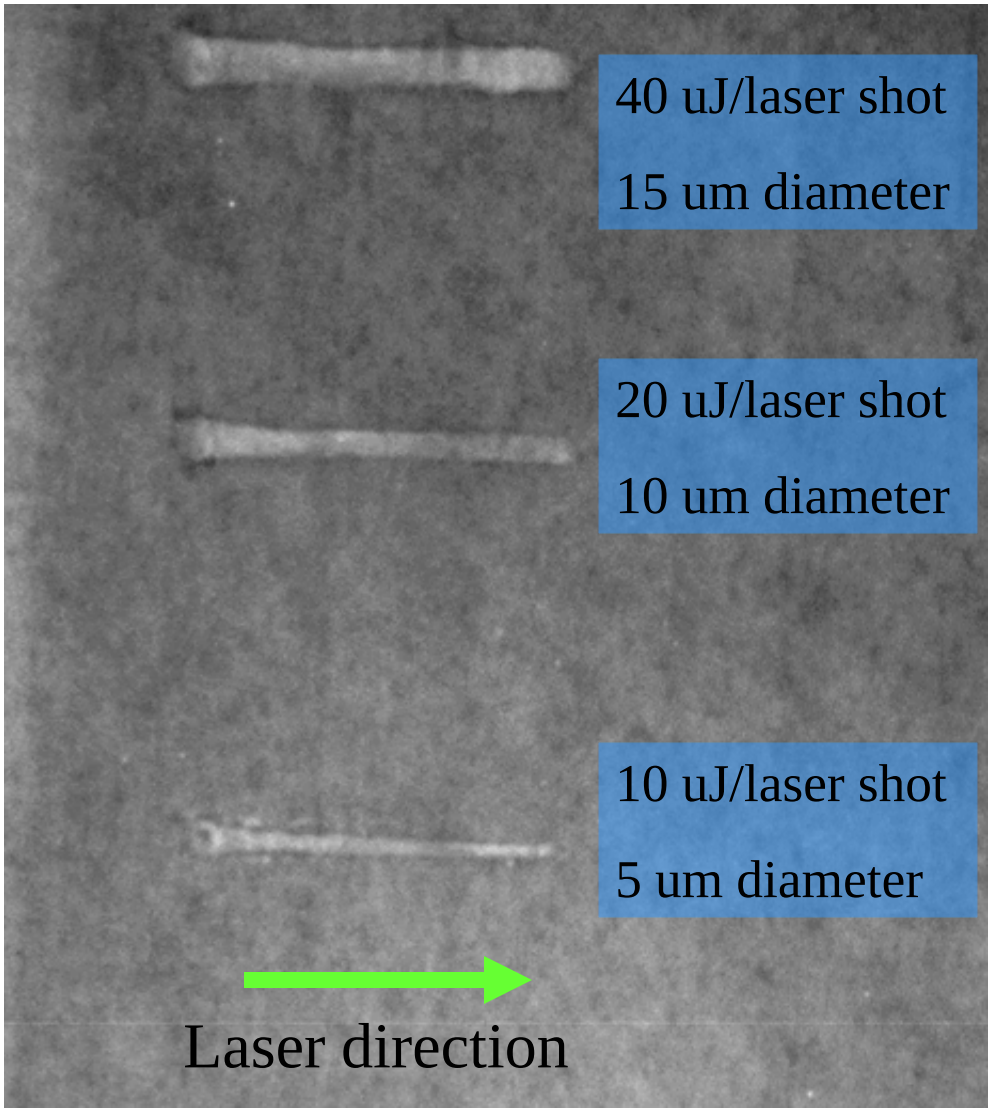

We can manipulate warm dense matter to improve the situation.

- **Substantial effort is often made to reduce laser-plasma interaction**
  - Femtosecond lasers
  - Gas assist jets

- **Double pulse format uses ablation products.**
  - Nanosecond lasers

- **Improvement in speed and quality.**

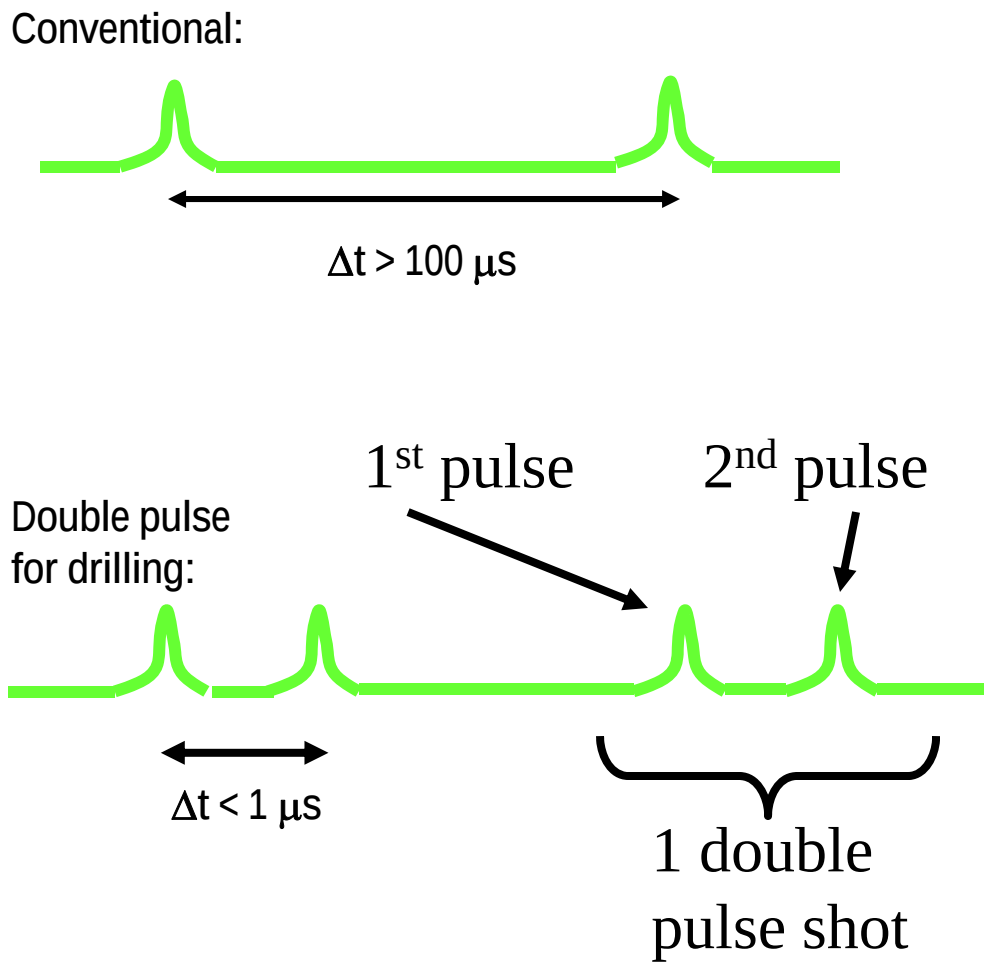

Why use double pulse ?

Double pulse machining improves the speed of percussion drilling.

- Enhances basic material removal rate.
- Improves ejection of ablation products

- laser:
  - τ=4 ns,
  - λ=532 nm,
  - up to 3 mJ/pulse

$$5\times10^{9} < \Phi_L < 10^{11} \quad W/cm^2$$

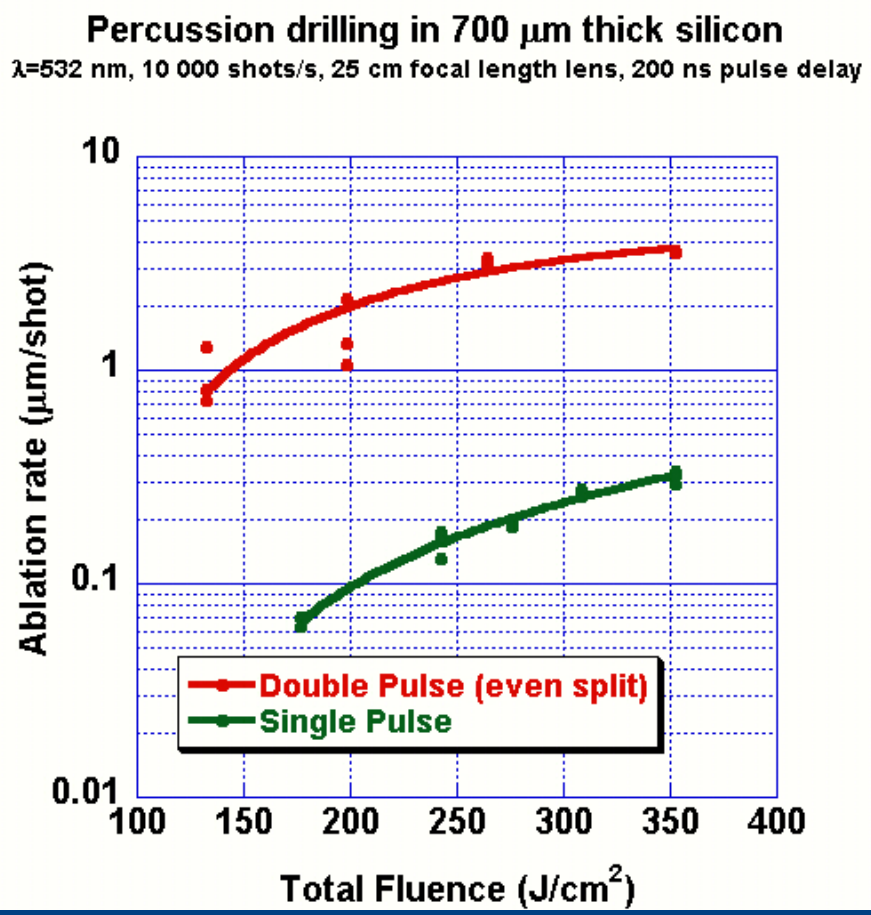

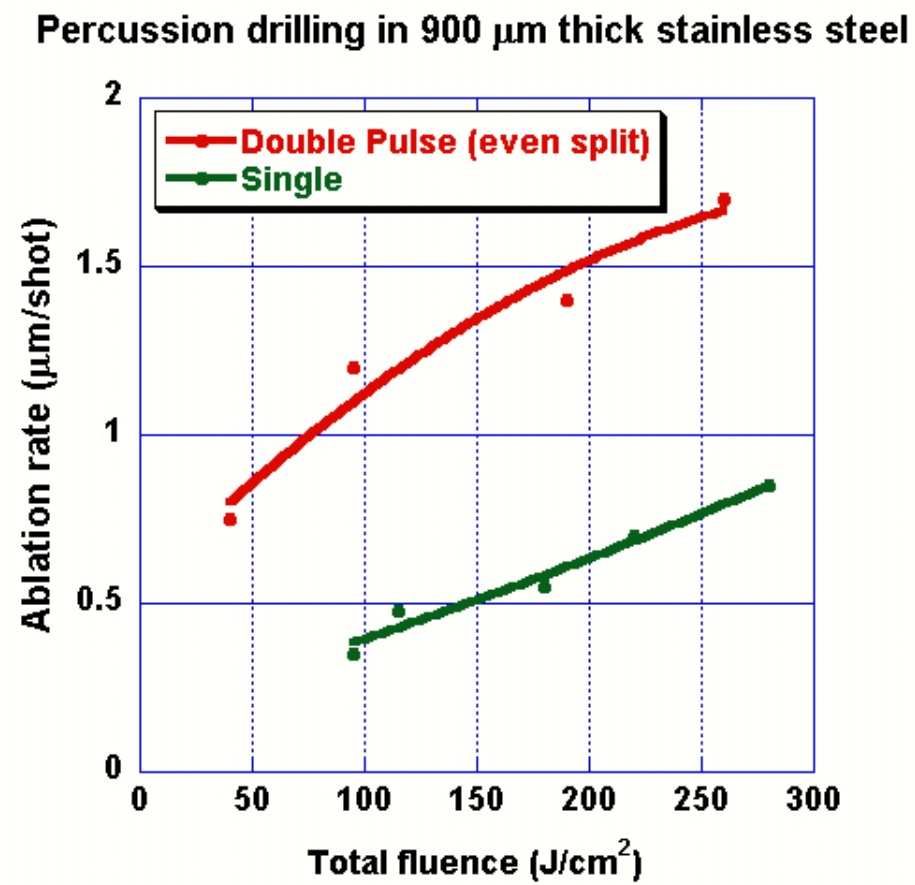

Why use double pulse ? Double Pulse machining improves the quality of percussion drilled holes.

- **Double pulse format can reliably percussion drill high aspect holes.**

800 shots

Single pulse

1 mm thick stainless steel.

200 shots

Double pulse format

Basic behavior of double pulse machining forms a basis for a phenomenological model.

- **1st pulse produces:**
  - Hot plasma and post-shot ejecta
  - 30-60 kBar pressure
- **2nd pulse couples to residual WDM: the "dark cloud" and not the solid underneath**
  - Hot but enlarged plasma
  - 5-20 kBar pressure
  - Better and predictable holes
  - Much faster:
    - Weakly dependent on hole depth in steel.
    - Strongly dependent on hole depth in aluminum.
- **2 mechanisms at work.**

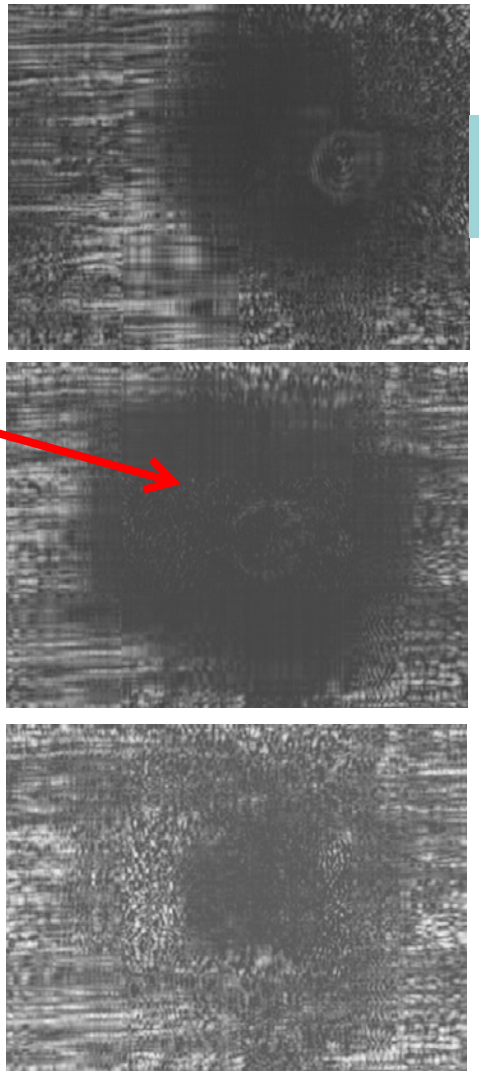

11 ns post-shot: plasma plume

37 ns post-shot: "stationary" dark material

30 seconds post-shot: laser damage.

Phenomenological model: improved ablation and inhibited redeposition.

- **Stage 1: 1st laser pulse.**
  - Produces high (30-50 kBar) pressures
  - Inhibits ablation.
- **Stage 2: Time delay.**
  - Boiling and evaporation continues.
  - Ablation plasma dissipates
  - **"Low" temperature cloud remains**.
- **Stage 3: 2nd laser pulse**
  - Heats dark cloud (10-20 eV)
  - Interacts with larger volume.
  - Produces thermal heat source without confining pressure (PV=nRT)
  - Ablation proceeds rapidly (>6X)
  - Inhibits redeposition

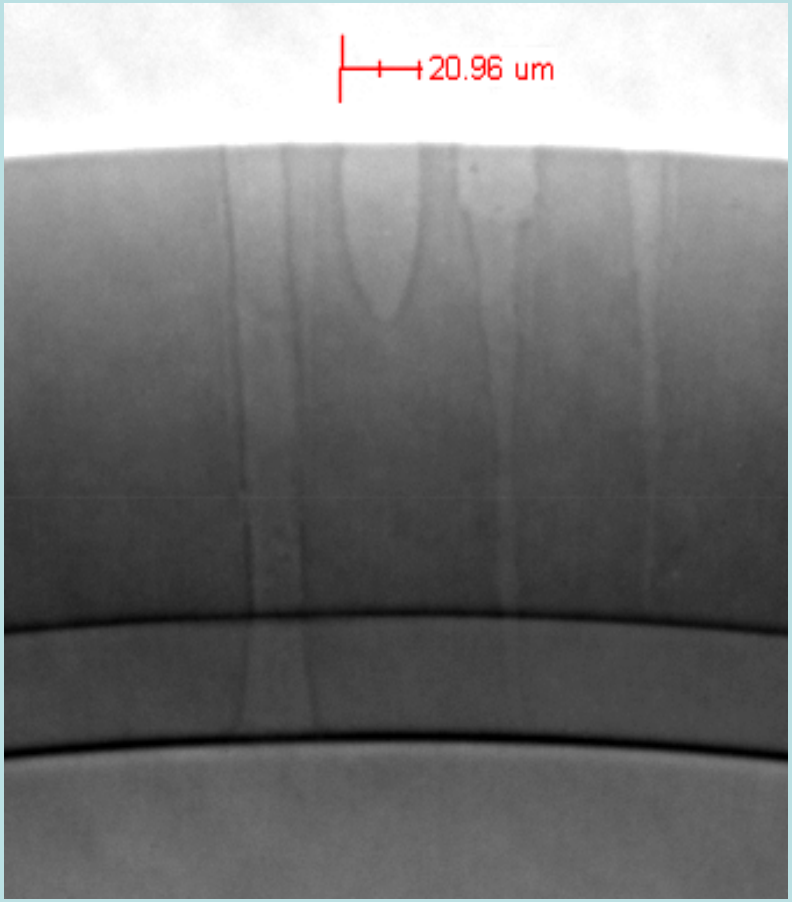

We can manipulate these processes.

We are learning to simulate what the second laser pulse hits and what state the laser thus creates

- Ionization for the 1/100th-1/5th solid density
- Te from .3 eV to 20 eV.
- Permits us to model the deposition of the secondary pulse in the low temperature dark cloud.

Underlying Mechanism of DP Laser Drilling May Involve Manipulating the Process Paths in the ρ-T Phase Diagram

- **Process paths for the expanding warm-dense matter following first laser strike on Aluminum, Φ_{laser} ~ 10 -100 J/cm^2**

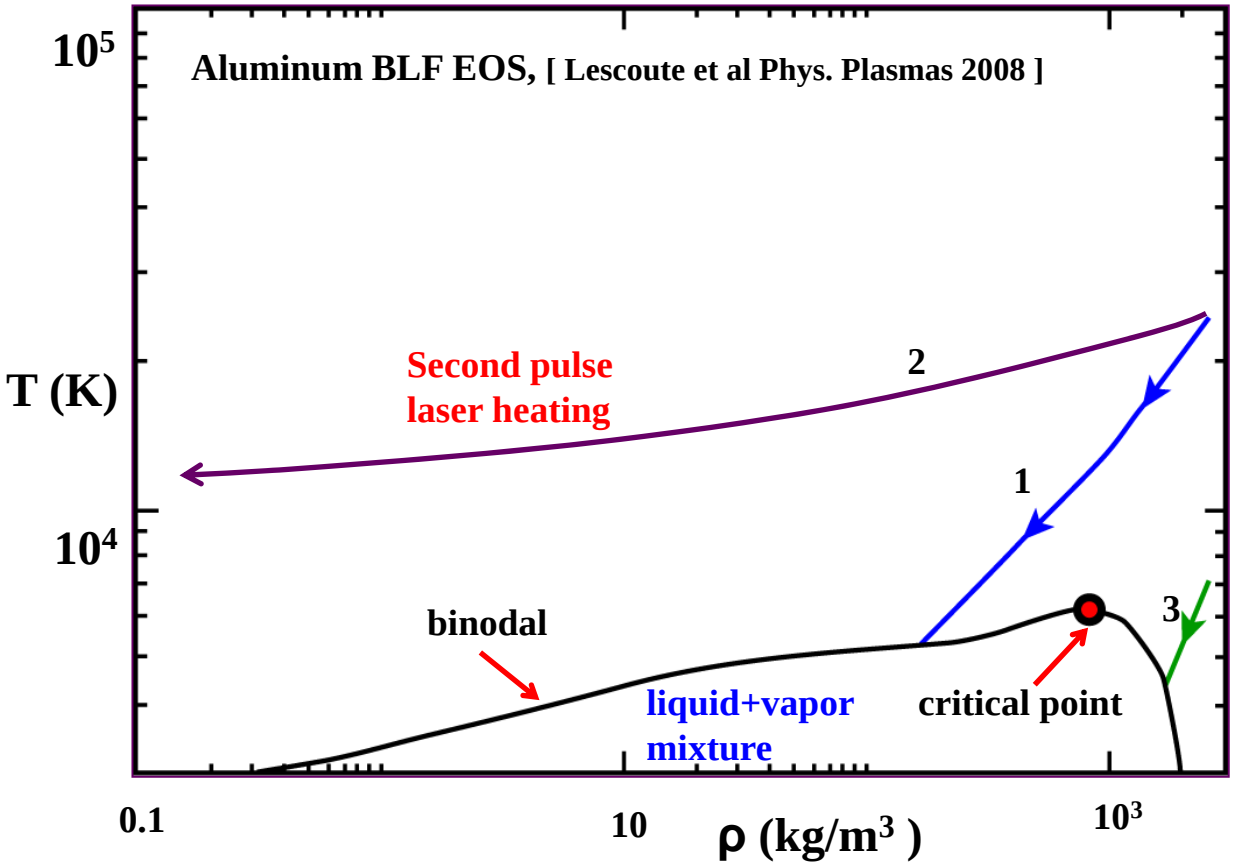

- **Process 1: Expansion is adiabatic: Path crosses the liquid-vapor binodal: result is dynamic recondensation with possible recast.**

- **Process 2: Expansion is accompanied by second pulse heating: material remains in the gas phase above the binodal: no chance of recondensation.**

- **Process 3: Pressure release causes expansion of hot liquid phase underneath cold cloud. Liquid converts to gas bubbles after intersecting the binodal: recondensation unlikely.**

Recall the 1 ns pulse….

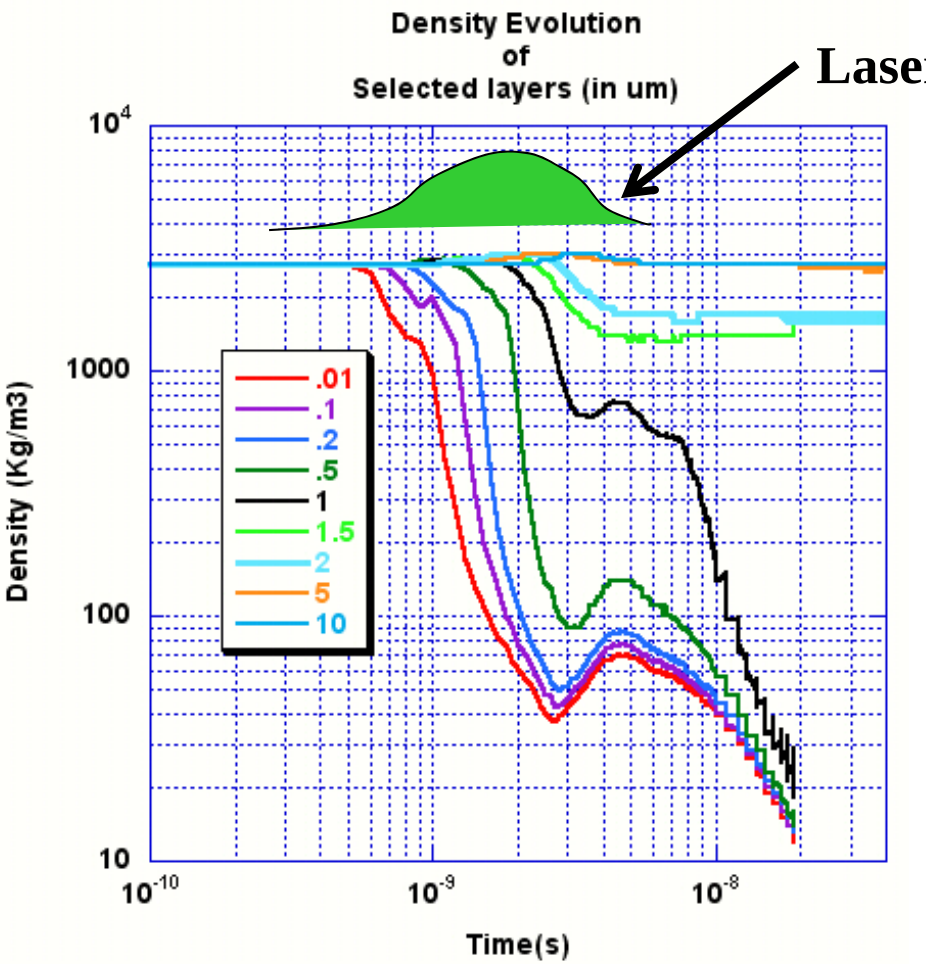

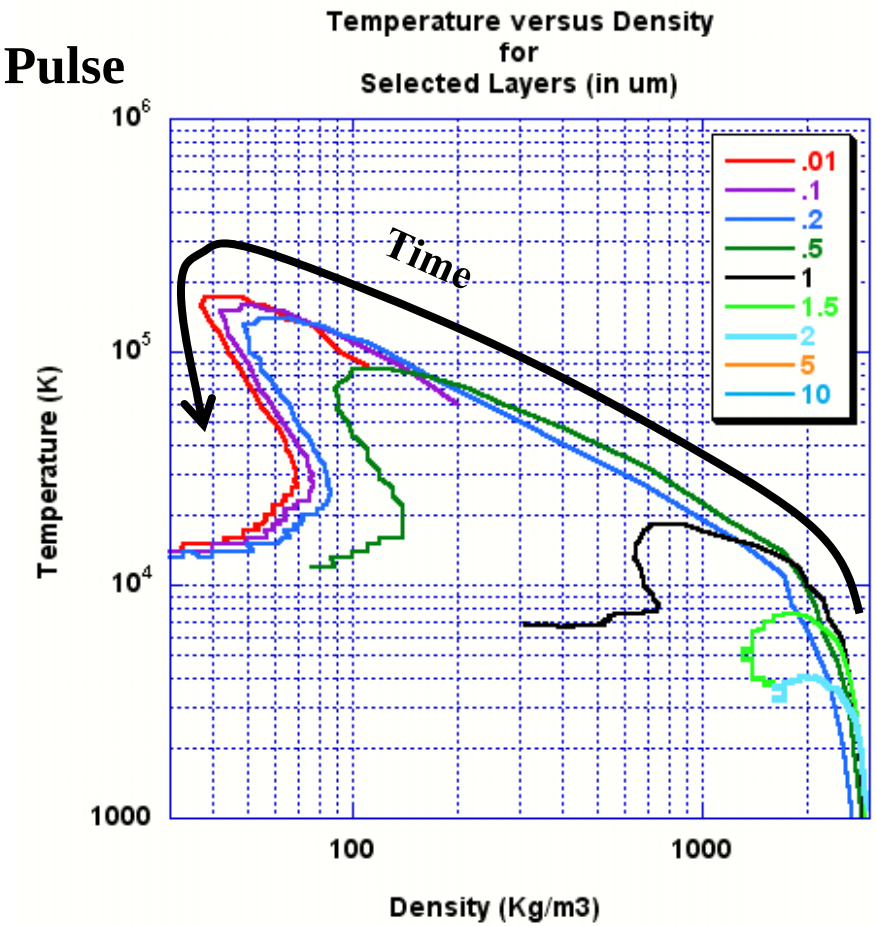

$$\left(2\times10^{11}\,W/cm^{2}\right)$$

Charge-State Ionization Fractions as Function of Temperature for Dense Non-Ideal Aluminum Plasmas

- **Solved coupled set of Saha equations supplemented by electro-neutrality and a semi-empirical expression for lowering ΔI_z of the ionization energies I_z (pressure ionization). Simple model captures electrical properties of hot expanded metal-nonmetal transition fairly well.**
  - **Charge State fractions α_z at fixed density ρ = 200 kg/m^3 agree well with Pade approximations for interaction parts of chemical potentials [Kuhlbrodt and Redmer (2000)].**

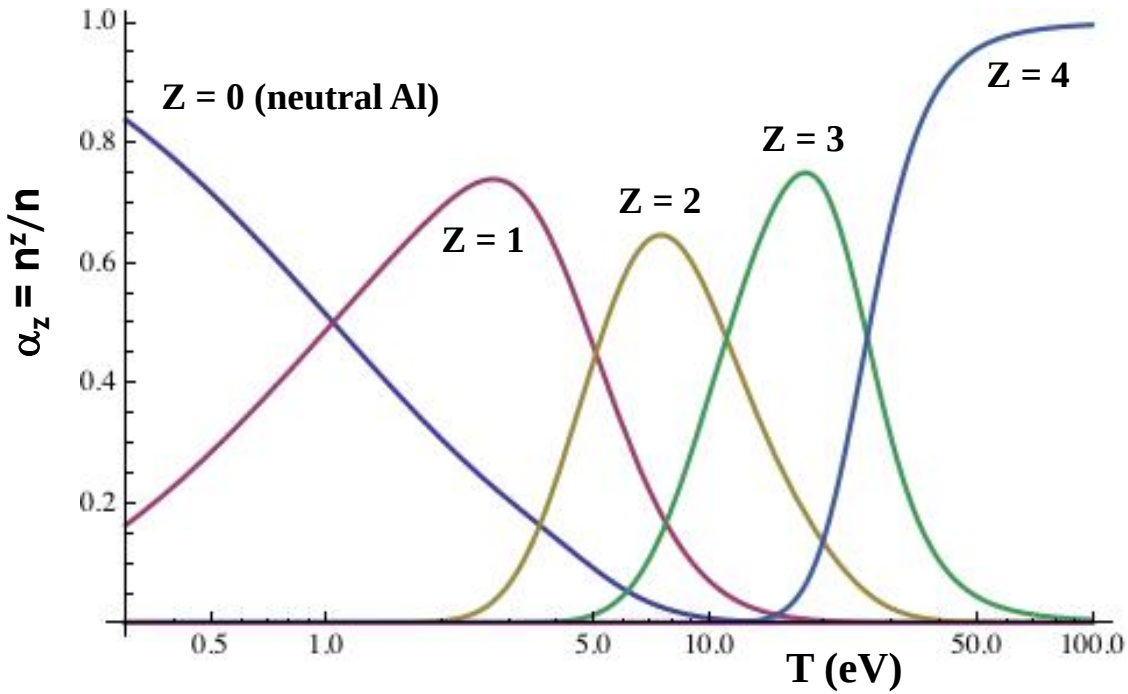

$$\frac{-\Delta I_z}{I_z} = \left(\frac{3e^2}{2r_s I_z}\right)^{3/2}$$

– **Desjarlais (2001)**

$$\frac{-\Delta I_z}{I_z} = \frac{e^2}{r_s I_z}\left(0.8\bar{Z} + 2.51\right)$$

– **Basko et al (1997)**

$$r_s = \left(\frac{3}{4\pi n}\right)^{1/3}$$ – **Wigner-Seitz radius**

$\bar{Z} = n_e / n$ – **Ionization degree**

Laser Absorption Determined from Various Models Used for Plasma Optical Properties in Warm Dense Matter Regimes

- **Apply linear response theory to average-atom version of the Kubo-Greenwood formula for the optical conductivity Re[σ(ω)] = J(ω)/E(ω), where J(ω) is in-phase current associated with perturbed electron motions: Includes free-free, bound-free (photo) and bound-bound (line) transitions [Johnson et al JQS (2006)]**

- **Complex dielectric constant** $\varepsilon(\omega) = 1 + i\dfrac{4\pi\sigma(\omega)}{\omega}$ $\quad \sigma(\omega) = \mathrm{Re}\,\sigma(\omega) + i\,\mathrm{Im}\,\sigma(\omega)$
  - **Kramers-Kronig relation determines imaginary part**

- **Tractable form invokes "effective" electron collision frequency ν_{eff} (v) and a normalized unperturbed Fermi-Dirac free electron distribution f_0 (v)**

$$\varepsilon(\omega) = 1 + \omega_{pe}^2 \int \frac{\mathrm{v}}{3}\frac{\partial f_0}{\partial \mathrm{v}}\frac{(1 - i\nu_{eff}/\omega)}{(\omega^2 + \nu_{eff}^2)} d^3\vec{\mathrm{v}} \approx 1 - \omega_{pe}^2 \frac{(1 - i\bar{\nu}_{eff}/\omega)}{(\omega^2 + \bar{\nu}_{eff}^2)}$$

(Familiar Drude-like form)

$$\frac{1}{\bar{\nu}_{eff}} = \frac{1}{\nu'} + \frac{1}{\nu_{e-ph}}$$

Modified "temperature" accounts for degeneracy heuristically

$$\nu' = \nu_{ei}(T_*) + \nu_{en}(T_*)$$

$$T_* = (T^2 + gE_{Fermi}^2)^{1/2} \quad (g \sim 1)$$

Smoothed joining expression [Benuzzi-Huller-Eidmann (1998)] is good in vicinity of metal-nonmetal transition where electron-phonon collisions dominate at low T high ρ with corresponding weaker collision frequency

$$\nu_{e-ph} = \frac{\mathrm{const}\; c_s^2}{a_{Bohr}\,\mathrm{v}_{Fermi}}$$

const chosen to fit cold DC metallic σ (ω = 0)

Description of Laser Absorption Model cont'd

- **Electron-ion collision rate** Debye screening breaks down in dense strongly coupled plasma regime so Spitzer-Harm form has to include ion-ion correlation correction to avoid diverging Coulomb logarithm [Benuzzi et al 1998, Kim and Kim, 2003]

$$\nu_{ei}(\rho,T) = \frac{4e^4 n \ln[1+\Lambda^2(\omega)]^{1/2}}{3T_*^{3/2}} \left(\frac{2\pi}{m_e}\right)^{1/2} \sum_z Z^2 \alpha_Z \qquad \Lambda(\omega) = \frac{b_{\max}}{b_{\min}} \qquad \begin{aligned} b_{\max} &= \min\left(\mathrm{v}_{te}/\omega_{pe},\ \mathrm{v}_{te}/\omega\right) \\ b_{\min} &= \max\left(\bar{Z}e^2/m_e \mathrm{v}_{te}^2,\ \hbar/\mathrm{v}_{te} m_e\right) \end{aligned}$$

- **Electron-neutral collision rate** $\nu_{en}(\rho,T) = \mathrm{v}_{te} n_0 Q_{e0}(n_e,T)$
  - The electron neutral momentum transfer cross section used a screened polarization potential with screening length of arbitrary degeneracy, reproducing the Debye length $\lambda_D = \mathrm{v}_{te}/\omega_{\mathrm{pe}}$ in the low-density classical limit. [Desjarlais 2001,Kim and Kim 2003].
  - Typical value for ~ 1 eV sub-solid density Al plasmas is $Q_{e0} \sim (2-35)\times 10^{-15}\ \mathrm{cm}^2$ can exceed the Lee and More ad hoc cross section by ~ 10x, and is needed to explain minimum in DC electrical conductivity at T ~ 1 eV and ρ ~ 30 kg/m³ [DeSilva and Katsouros, 1998].

- **Complex Index of refraction** $n + i\kappa = \sqrt{\varepsilon(\omega)} = \sqrt{\mathrm{Re}\,\varepsilon(\omega) + i\,\mathrm{Im}\,\varepsilon(\omega)}$

$$\begin{pmatrix} n \\ \kappa \end{pmatrix} = 2^{-1/2}\sqrt{[(1-\psi)^2 + \lambda^2\psi^2]^{1/2} \pm (1-\psi)} \qquad \psi = \frac{n_e}{n_{ecrit}} \frac{1}{(1+\lambda^2)}, \qquad \lambda = \frac{\nu_{eff}}{\omega}$$

- **Laser power flux attenuation** $\dfrac{dI}{dx} = -2k_{abs} I, \quad k_{abs} = k_0\kappa \ \ (k_0 = \omega/c = 1.18\times 10^7\,\mathrm{m}^{-1})$

Real $n(\omega)$ and Imaginary $\kappa(\omega)$ parts of Index of Refraction for 532 nm Laser Light in Al Plasma

- Strict wave cutoff ($n \rightarrow 0$) prevented at critical surface ($\omega=\omega_{pe}$) because of high ν_{eff}. Still, at $\omega = \omega_{pe}$ the dip in n deepens for higher T because ν_{eff} is getting lower.

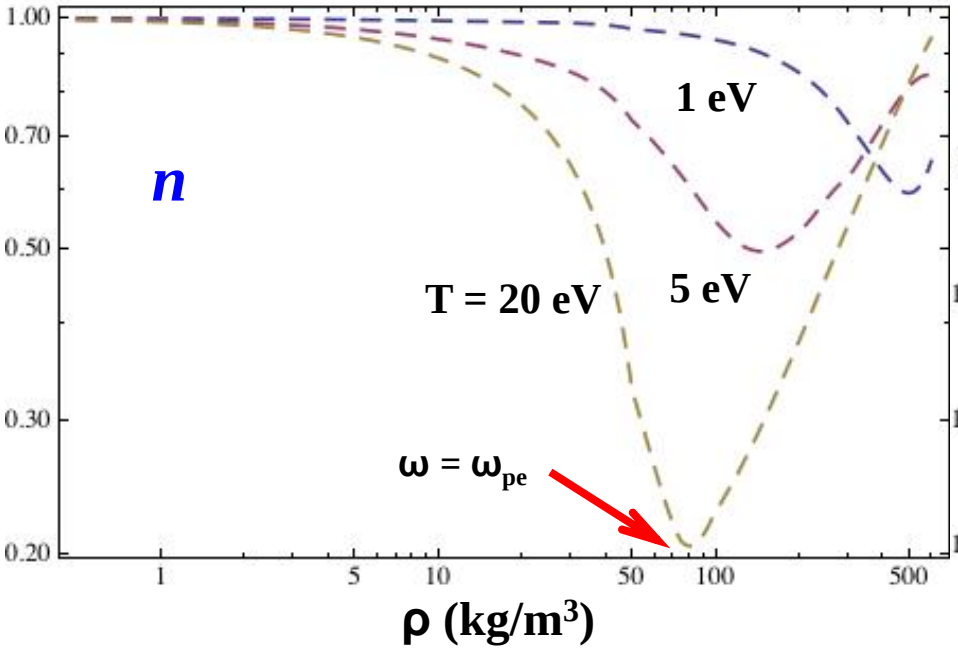

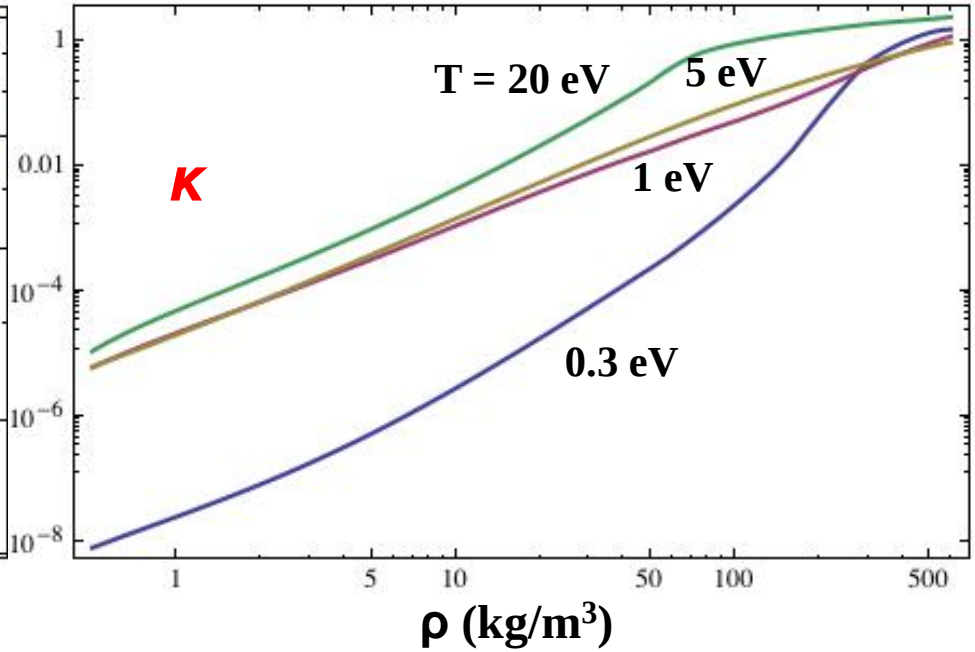

- Power absorption skin thickness $\delta = c/(2\omega\kappa)$ in, dense "cold dark cloud" $\rho > 50$ kg/m^3, varies from 2μm < δ <100μm for T ≤ 1 eV. Could a thicker, and thus more spatially uniform absorbing layer in the cold cloud act to "cushion" the target and lower target pressure during second laser strike?

These models will permit us to model the interaction of the laser with the dark cloud

- **Will we still see the 2 mechanisms postulated in the phenomenological model ?**
- **Will the laser heating drive enough of the dark cloud into a temperature range where thermal conductivity is strong ?**
  - Enhanced ablation
- **Will enough of the dark cloud be heated so that it does not redeposit ?**

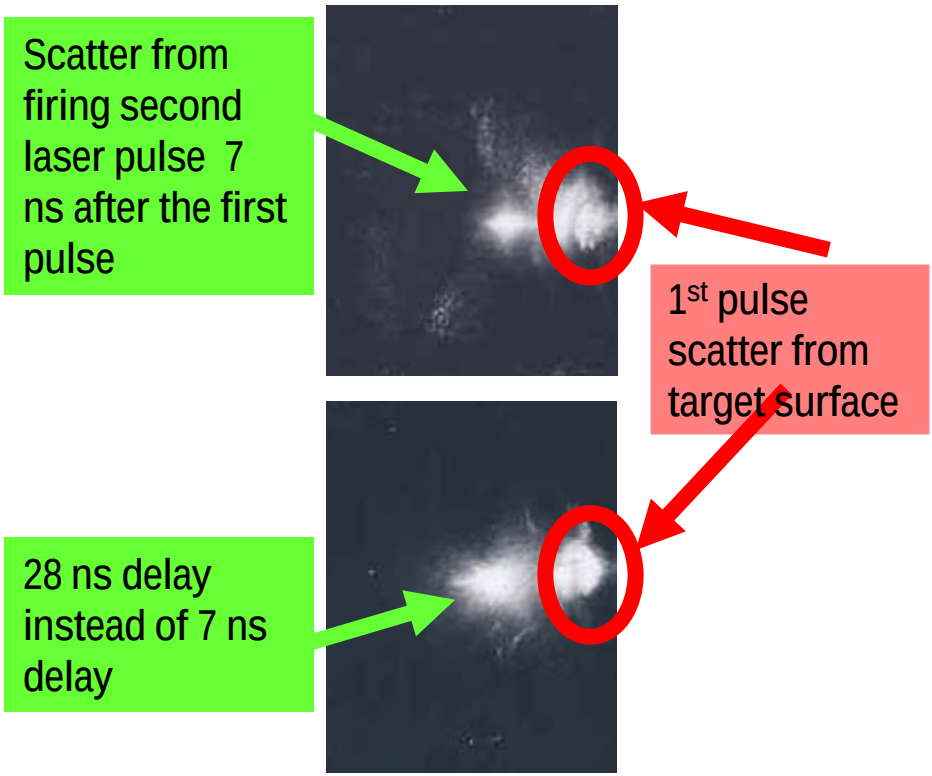

Now we see how WDM contributes to laser machining, how can ion beams enable further work ?

- **Temporally and Spatially localized measurements of WDM (for transport properties).**

- **Heavy ion beam driven foils are uniformly heated.**

- **The conditions can be created on timescales that are convenient for doing experiments.**
  - All we need is a way to capture and hold the expanding plasma long enough to measure it.
  - Not tamping.

- **We do this in a 2-step process:**

Step 1: Explode a thin foil with an ion beam, optically measure Reflectivity and Transmission

Ref and Trans can yield σ_{ac}

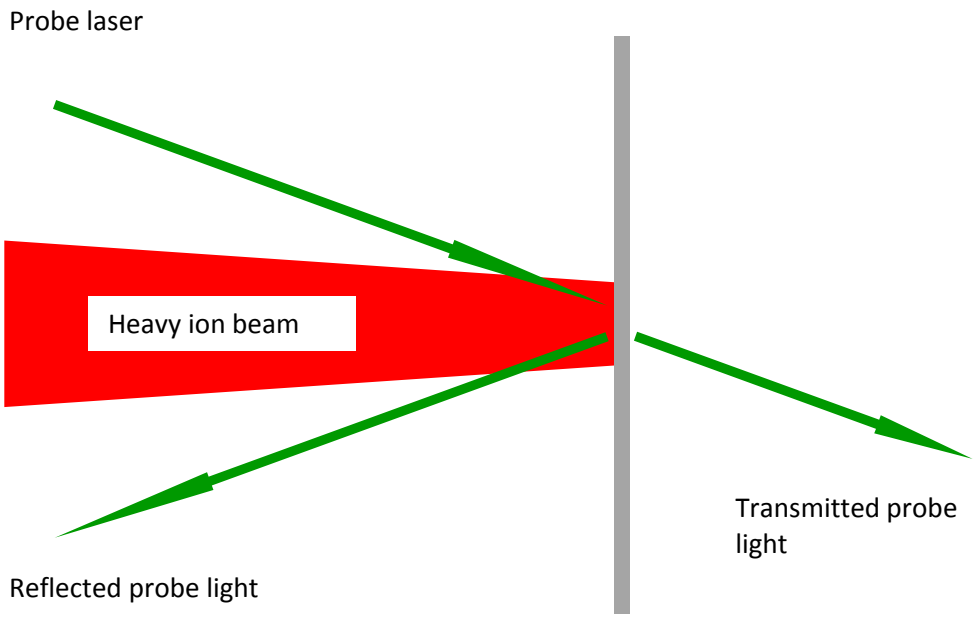

Thin target foil

100 Å ≤ thickness ≤1 µm

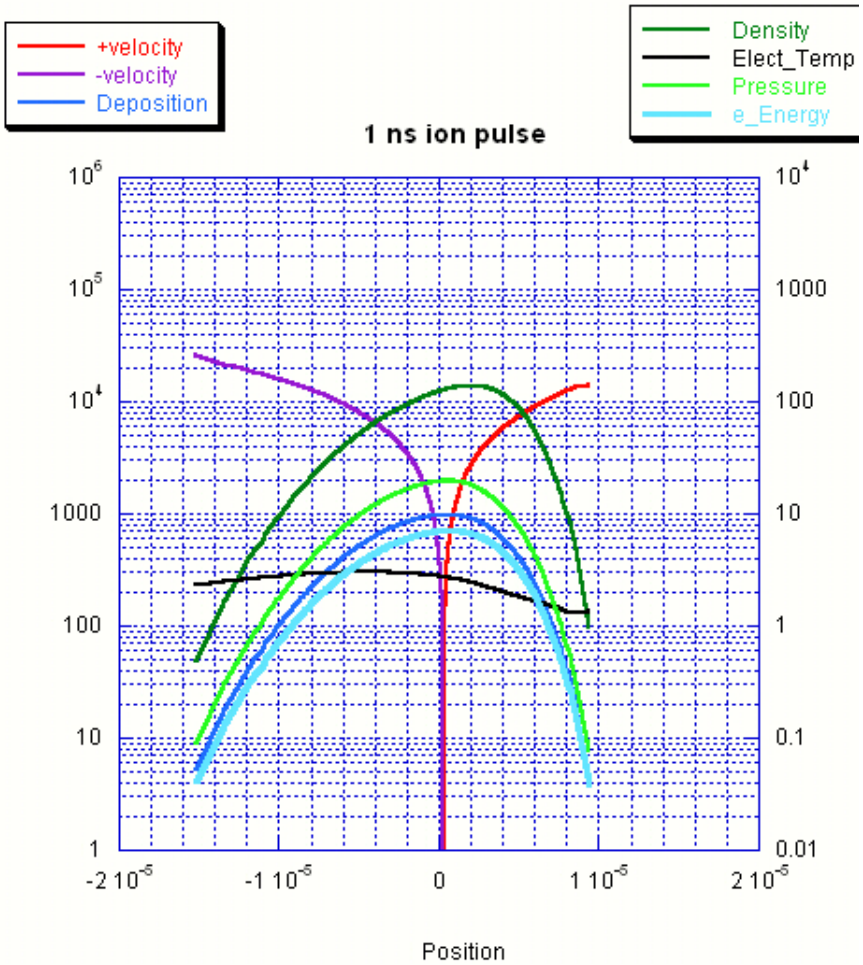

Problem: Gradients in ρ and T

A possible solution is to use a grid of tapered holes to catch the plasma.

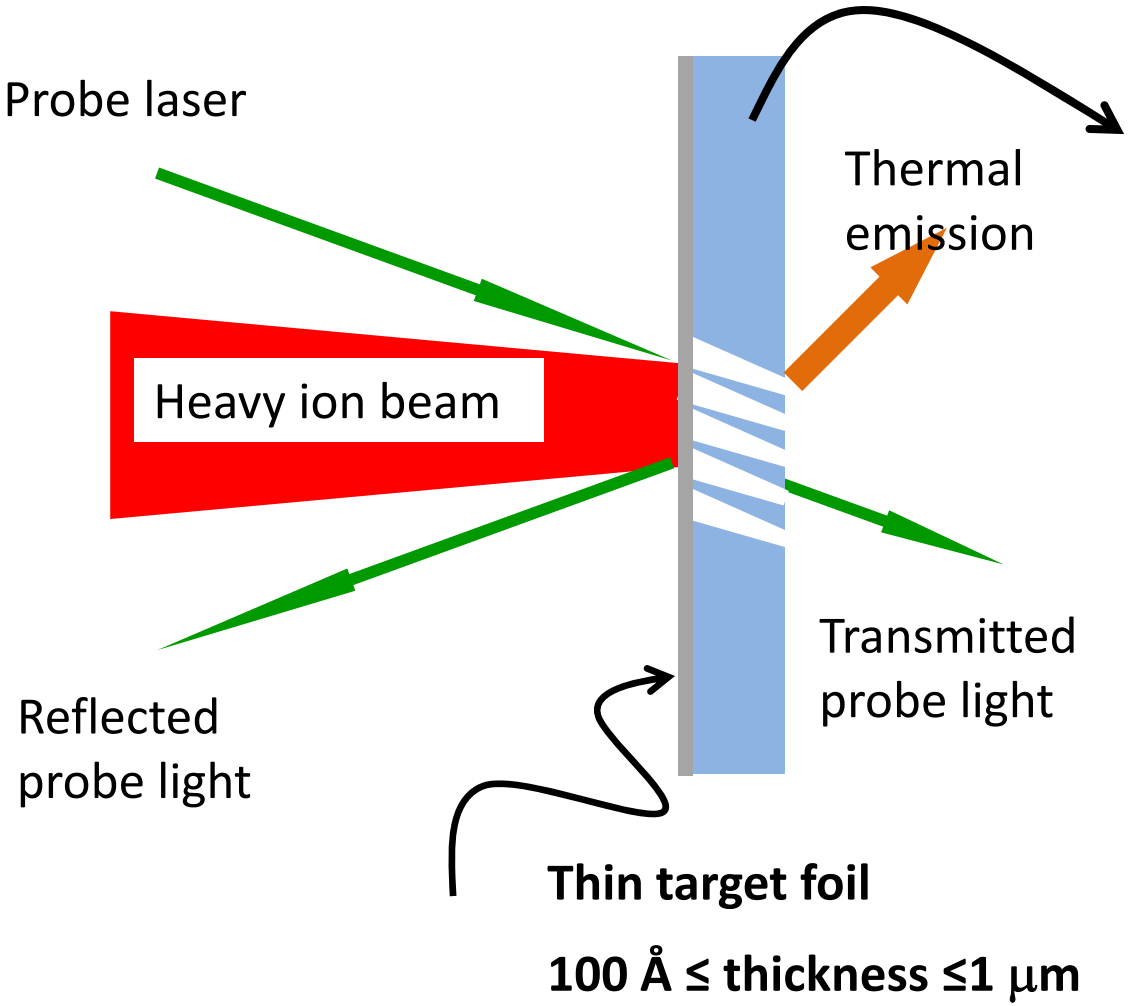

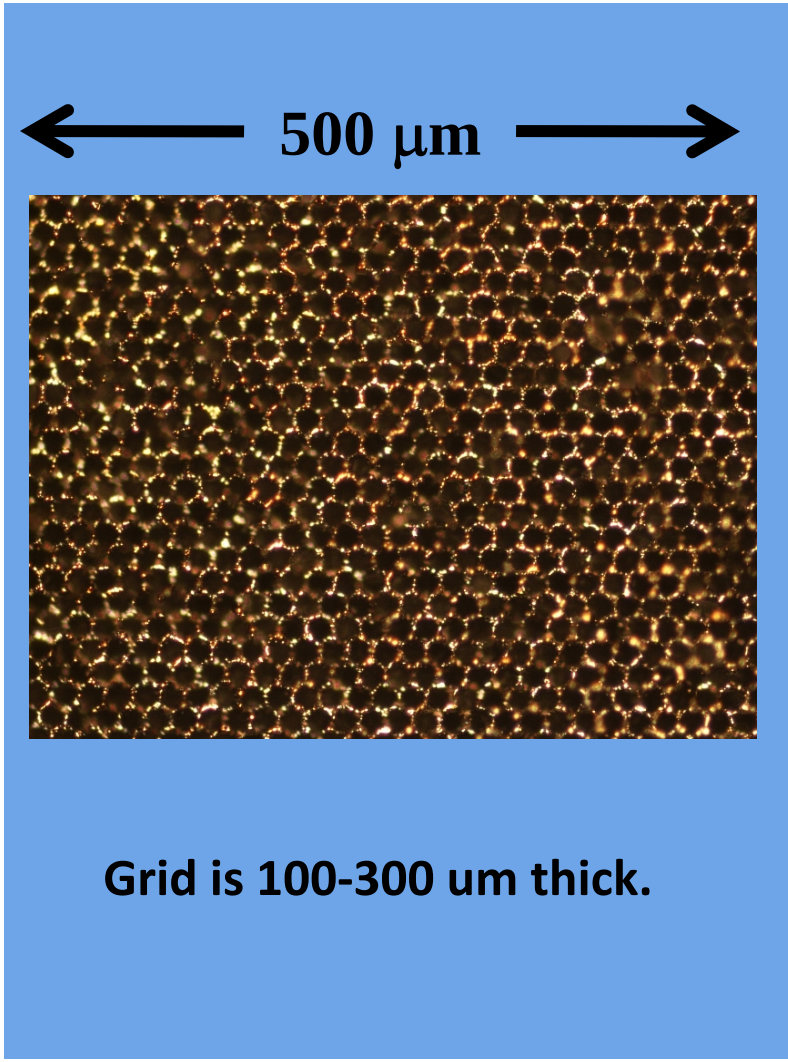

The array of tapered holes is intended to provide a soft stop for the plasma to reduce secondary shocks as well as restricted 1-D expansion

- **Grid of tapered holes:**
  - 15 um tapered to 5 um
  - 100 um -300 um deep.
  - Close packed
  - Entrance side is nearly open
  - Spatial resolution for imaging diagnostics

- **Plasma expansion becomes asymmetric after 10X expansion ?**
  - 1-D and restricted expansion in grid.
  - Open side blows away rapidly to allow good optical access.

- **Limited mass targets can help ?**

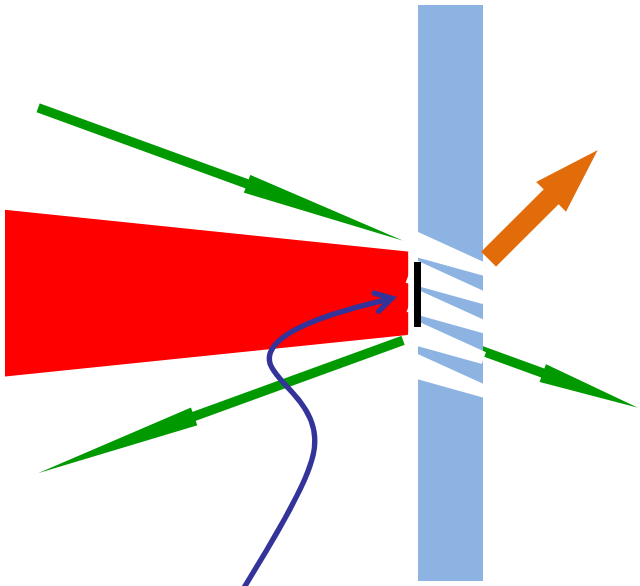

Thin target foil

"small" diameter

Actual modeling of the effect of the grid of tapered holes needs to be done.

- **Preliminary attempt using a planar hydrocode.**
  - Gradients strongly reduced.
  - Quasistatic.
  - Expect actual grid to be much better.
- **Fixed boundary 50 um to right of a 0.5 um thick AL target.**
  - Mock-up of 100 um deep grid with 50% volume removed.
- **Target is heated for 1 ns at 10 J/cm^2 by a heavy ion beam**

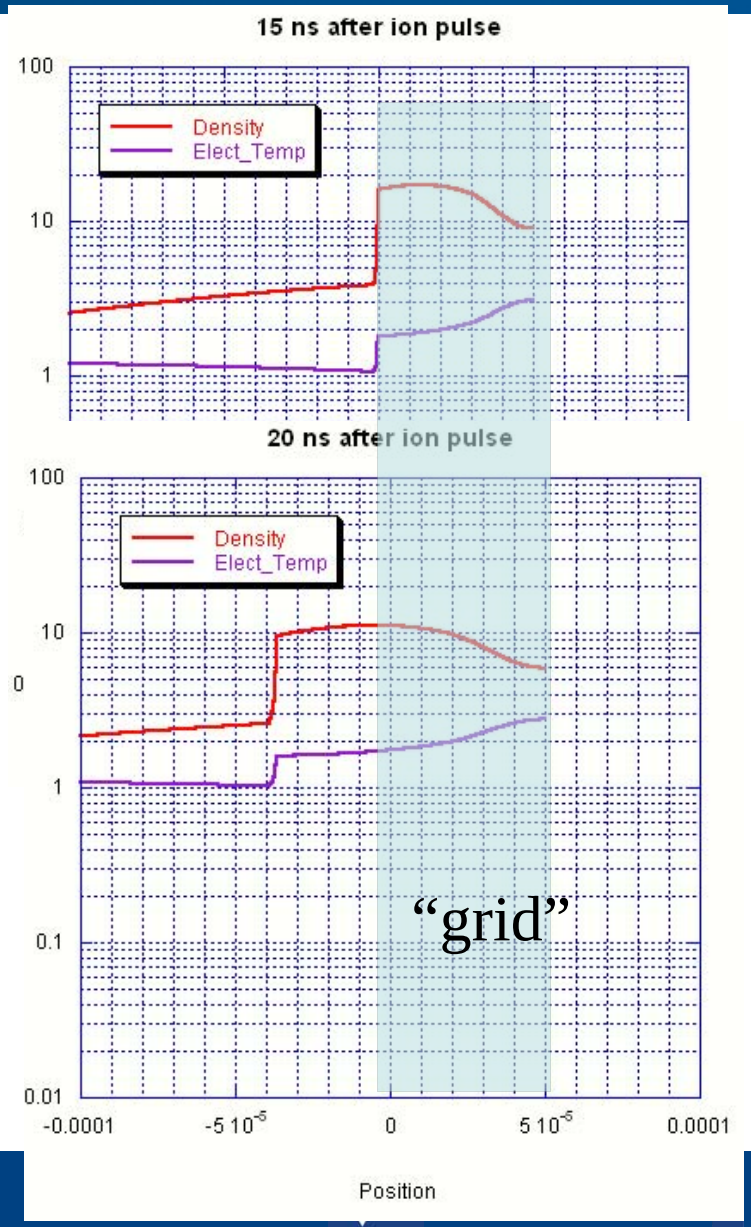

Conclusions

- **WDM is present in much of laser materials processing.**
  - LMP does not end with the laser pulse.

- **Improved modeling of the relevant WDM explains phenomena observed in laser machining.**
  - Will continue to lead to better manipulation of WDM (pulse formatting) in LMP.
  - > $10B industry that will grow.

- **Combining optical diagnostics and microstructured surfaces with pulsed ion beam driven targets may yield spatially and temporally localized measurements of EOS and transport of WDM.**